Running Title:

"ER-Ca^{2+} sensor STIM regulates neuropeptides required for development under nutrient restriction in *Drosophila*"

Megha*(1), Christian Wegener (2) and Gaiti Hasan(1)

1. National Centre For Biological Sciences, Tata Institute for Fundamental Research, Bellary Road, Bangalore 560065
2. Department of Neurobiology and Genetics, Theodor-Boveri-Institute, Biocenter, University of Würzburg, Am Hubland, 97074 Würzburg

*Corresponding author; Contact: meghaphd@ncbs.res.in

ORCID:

Megha: 0000-0002-2968-8211

Christian Wegener: 0000-0003-4481-3567

Gaiti Hasan: 0000-0001-7194-383X

Abstract

Neuroendocrine cells communicate via neuropeptides to regulate behaviour and physiology. This study examines how STIM (Stromal Interacting Molecule), an ER-Ca^{2+} sensor required for Store-operated Ca^{2+} entry, regulates neuropeptides required for *Drosophila* development under nutrient restriction (NR). We find two STIM-regulated peptides, Corazonin and short Neuropeptide F, to be required for NR larvae to complete development. Further, a set of secretory DLP (Dorso lateral peptidergic) neurons which co-express both peptides was identified. Partial loss of *dSTIM* caused peptide accumulation in the DLPs, and reduced systemic Corazonin signalling. Upon NR, larval development correlated with increased peptide levels in the DLPs, which failed to occur when *dSTIM* was reduced. Comparison of systemic and cellular phenotypes associated with reduced *dSTIM*, with other cellular perturbations, along with genetic rescue experiments, suggested that *dSTIM* primarily compromises neuroendocrine function by interfering with neuropeptide release. Under chronic stimulation, *dSTIM* also appears to regulate neuropeptide synthesis.

Introduction

Metazoan cells commonly use ionic Ca^{2+} as a second messenger in signal transduction pathways. To do so, levels of cytosolic Ca^{2+} are dynamically managed. In the resting state, cytosolic Ca^{2+} concentration is kept low and maintained thus by the active sequestration of Ca^{2+} into various organelles, the largest of which is the ER. Upon activation, ligand-activated Ca^{2+} channels on the ER, such as the ryanodine receptor or inositol 1,4,5-trisphosphate receptor (IP_3R), release ER-store Ca^{2+} into the cytosol. Loss of ER-Ca^{2+} causes STromal Interacting Molecule (STIM), an ER-resident transmembrane protein, to dimerize and undergo structural rearrangements. This facilitates the binding of STIM to Orai, a Ca^{2+} channel on the plasma membrane, whose pore now opens to allow Ca^{2+} from the extracellular milieu to flow into the cytosol. This type of capacitative Ca^{2+} entry is called Store-operated Ca^{2+} entry (SOCE) [1]. Of note, key components of SOCE include the IP_3R, STIM and Orai, that are ubiquitously expressed in the animal kingdom, underscoring the importance of SOCE to cellular functioning. Depending on cell type and context, SOCE can regulate an array of cellular processes [2].

Neuronal function in particular is fundamentally reliant on the elevation of cytosolic Ca^{2+}. By tuning the frequency and amplitude of cytosolic Ca^{2+} signals that are generated, distinct stimuli can make the same neuron produce outcomes of different strengths [3]. The source of the Ca^{2+} influx itself contributes to such modulation as it can either be from internal ER-stores or from the external milieu, through various activity-dependent voltage gated Ca^{2+} channels (VGCCs) and receptor-activated Ca^{2+} channels or a combination of the two. Although the contributions of internal ER-Ca^{2+} stores to neuronal Ca^{2+} dynamics are well recognized, the study of how STIM and subsequently, SOCE-mediated by it, influences neuronal functioning, is as yet a nascent field.

Mammals have two isoforms of STIM, STIM1 and STIM2, both which are widely expressed in the brain. As mammalian neurons also express multiple isoforms of Orai and IP_3R, it follows that STIM-mediated SOCE might occur in them. Support for this comes from studies in mice, where STIM1-mediated SOCE has been reported for cerebellar granule neurons [4] and isolated Purkinje neurons [5], while STIM2-mediated SOCE has been shown in cortical [6] and hippocampal neurons [7]. STIM can also have SOCE-independent roles in excitable cells, that are in contrast to its role via SOCE. In rat cortical neurons [8] and vascular smooth muscle cells [9], Ca^{2+} release from ER-stores prompts the translocation of STIM1 to ER-plasma membrane junctions, and binding to the L-type VGCC, $Ca_V1.2$. Here STIM1 inhibits $Ca_V1.2$ directly and causes it to be internalized, reducing the long-term excitability of these cells. In cardiomyocyte-derived HL1 cells, STIM1 binds to a T-type VGCC, $Ca_V1.3$, to manage Ca^{2+} oscillations during contractions [10]. These studies indicate that STIM regulates cytosolic Ca^{2+} dynamics in excitable cells, including neurons and that an array of other proteins determines if STIM regulation results in activation or inhibition of neurons. Despite knowledge of the expression of STIM1 and STIM2 in the hypothalamus (Human Protein Atlas), the major neuroendocrine centre in vertebrates, studies on STIM in neuroendocrine cells are scarce. We therefore used *Drosophila melanogaster (Drosophila),* the vinegar fly, to address this gap.

Neuroendocrine cells possess elaborate machinery for the production, processing and secretion of neuropeptides (NPs), which perhaps form the largest group of evolutionarily conserved signalling agents [11,12]. Inside the brain, NPs typically modulate neuronal activity and consequently, circuits; when released systemically, they act as hormones. *Drosophila* is typical in having a vast repertoire of NPs that together play a role in almost every aspect of its behaviour and physiology [13,14]. Consequently, NP synthesis

and release are highly regulated processes. As elevation in cytosolic Ca^{2+} is required for NP release, a contribution for STIM-mediated SOCE to NE function was hypothesized.

Drosophila possess a single gene for STIM, IP_3R and Orai, and all three interact to regulate SOCE in *Drosophila* neurons [15,16]. In dopaminergic neurons, *dSTIM* is important for flight circuit maturation [15–17], with dSTIM-mediated SOCE regulating expression of a number of genes, including *Ral*, which controls neuronal vesicle exocytosis [17]. In glutamatergic neurons, *dSTIM* is required for development under nutritional stress and its' loss results in down-regulation of several ion channel genes which ultimately control neuronal excitability [18]. Further, *dSTIM* over-expression in insulin-producing NE neurons could restore Ca^{2+} homeostasis in a non-autonomous manner in other neurons of an IP_3R mutant [19], indicating an important role for dSTIM in NE cell output, as well as compensatory interplay between IP_3R and dSTIM. At a cellular level, partial loss of dSTIM impairs SOCE in *Drosophila* neurons [15,17,20] as well as mammalian neural precursor cells [21]. Additionally, reducing dSTIM in *Drosophila* dopaminergic neurons attenuates KCl-evoked depolarisation and as well as vesicle release [17]. Because loss of dSTIM specifically in $dimm^+$ NE cells results in a pupariation defect on nutrient restricted (NR) media [22], we used the NR paradigm as a physiologically relevant context in which to investigate STIM's role in NE cells from the cellular as well as systemic perspective.

Results

SOCE is required in sNPF and Crz producing cells for development under nutritional stress

Collectively, more than 20 different NPs are known to be made by the neuroendocrine cells in which reducing SOCE components resulted in poor pupariation upon NR [22]. To shortlist specific NPs important for this paradigm, we undertook a curated *GAL4-UAS*

104 screen. NP-GAL4s were used to drive the knockdown of *IP$_3$R* (*IP$_3$R^{IR}*) [23], and pupariation
105 of the resulting larvae were scored on normal vs NR media (Fig. S1A). On normal food, a
106 significant reduction of pupariation was seen only with *sNPF-GAL4* (Fig. S1A), whose
107 expression strongly correlates with neurons producing sNPF [24]. Upon NR, the largest
108 effect was seen with *sNPF-GAL4*, followed by small but significant pupariation defect with
109 *AstA-GAL4* and *DSK-GAL4* (Fig. S1A). Neurons that secrete NPs may also secrete
110 neurotransmitters, therefore, a role specifically for sNPF was tested. Reducing the level of
111 *sNPF* (*sNPF^{IR}*) or reducing an enzyme required for neuropeptide processing (*amontillado;*
112 *amon^{IR}*) [25] in *sNPF-GAL4* expressing cells, as well as a hypomorphic sNPF mutation
113 (*sNPF^{00448}*) resulted in impairment of larval development upon NR (Fig. S1B). These data
114 indicate that sNPF is required for pupariating under NR conditions.
115 *sNPF-GAL4* expresses in large number of neurons (>300) in the larval brain [24] (Fig.
116 S1C), and also expresses in the larval midgut and epidermis. To further refine sNPF$^+$
117 neurons on which we can perform cellular investigations, we tested a *Crz-GAL4* driver. This
118 driver expresses in fewer neurons (~22), all of which express the neuropeptide Corazonin
119 (Crz). Importantly, a small subset of these, three bilateral neurons in the brain lobe, make
120 Crz and sNPF. [24] (Fig. 1A). Reducing SOCE in Crz neurons, by reducing either IP$_3$R or STIM
121 (*dSTIM^{IR}*) [15,16] or over-expressing a dominant-negative version of Orai (*Orai^{E180A}*) [26],
122 resulted in reduced pupariation on NR (Fig. 1B). The absence of a developmental defect on
123 normal food suggests that SOCE in these neurons is primarily required to survive NR.
124 To test if both sNPF and Crz were required, they were specifically reduced (*sNPF^{IR}*;
125 *Crz^{IR}*) in Crz neurons. Knockdown of either NP resulted in larvae with a pupariation defect
126 on NR media but not, on normal food (Fig. 1C; Fig. S1D). In *Drosophila* neurons, enhancing
127 the expression of SOCE regulators leads to increased SOCE [16]. To test the positive effect

of SOCE on Crz and sNPF, a genetic compensation experiment was carried out. The SOCE-regulators, *IP_3R* or *dSTIM* were over-expressed in Crz neurons which also expressed reduced levels of either sNPF or Crz. NR larvae with this genetic make-up showed a significant improvement in pupariation on NR media, as compared to NR larvae with only reduced NPs (Fig. 1C). Interestingly, the compensation was sufficient to also increase the number of adults that emerged (Fig. 1D). Notably, over-expression of either of the two SOCE molecules, dSTIM and IP_3R on their own, did not affect pupariation on either normal or NR media (Fig. 1C), but unlike on normal food (Fig. S1E), did reduce development to adulthood on NR media (Fig. 1D). These data underscore the sensitivity of Crz neurons to ER-Ca^{2+} homeostasis during NR.

Loss of IP_3R and sNPF has previously been shown to affect larval feeding [27–29]. Hence, larval intake of dye-colored food in a 2-hour span was measured. Age-synchronized larvae with knockdown of either *dSTIM*, *IP_3R*, *Crz* or *sNPF* in Crz neurons exhibited no difference in the amount of dye ingested (Fig. S1F), suggesting that developmental defects in the NR assay do not arise from a fundamental feeding problem.

Altogether, these genetic experiments helped identify a set of NP expressing neurons, the Crz neurons, a subset of which also express sNPF, in which SOCE plays an important role during development on NR.

Figure 1

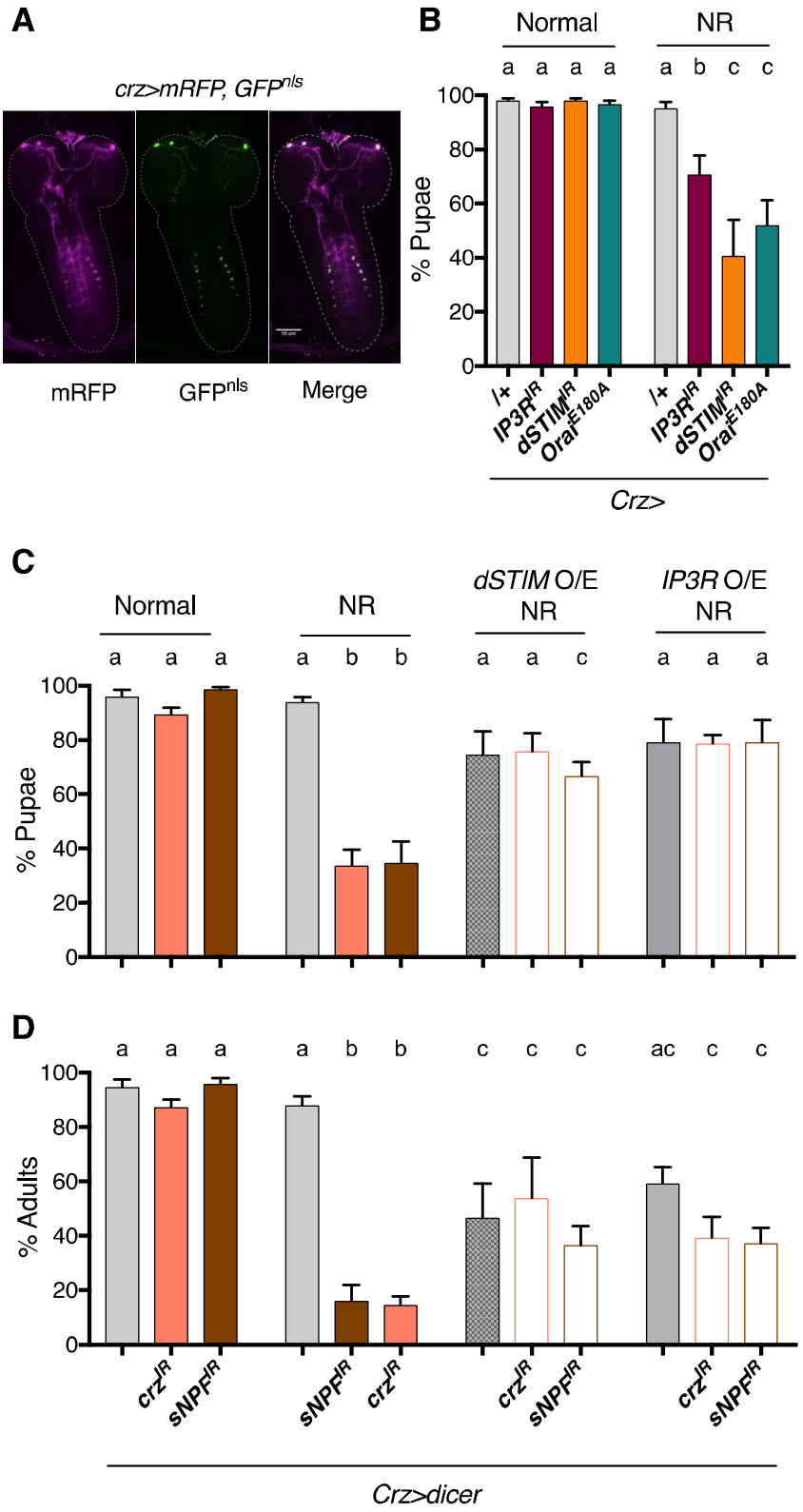

146

147 **Fig. 1 SOCE is required in Crz neurons for larval development on NR media. (A)**

148 Expression pattern of *Crz-GAL4* driver, used in this study to manipulate Crz neurons,

149 visualised by expressing membrane bound RFP (mRFP) and GFP with a nuclear localisation

150 signal (GFP^{nls}) **(B)** % Pupae upon reduction of SOCE by knockdown of *STIM* ($STIM^{IR}$), IP_3R

151 (IP_3R^{IR}) or ectopic expression of a dominant-negative *Orai* ($Orai^{E180A}$) in Crz neurons. To

152 measure pupariation, twenty five, 88h±3h old larvae, per vial, were transferred to either

153 normal food (corn flour, yeast, sugar) (See materials and methods for exact composition) or

154 nutrient restricted (NR; 100mM Sucrose) media and number of pupae (and adults where

155 relevant) that developed were counted. N = 6 vials for all experiments in this study. **(C)** %

156 Pupae upon reduction of either *sNPF* or *Crz* (Crz^{IR}, $sNPF^{IR}$) in Crz neurons, and when, *dSTIM*

157 or IP_3R are expressed in this background (*dSTIM* O/E; IP_3R O/E). **(D)** % Adults recovered for

158 genotypes in **(C)**. Bars with the same alphabet represent statistically indistinguishable

159 groups. Two-way ANOVA with Sidak multi comparison $p<0.05$ for (B), (C) and (D). See

160 also Figure Supplement 1.

161

Crz$^+$ and sNPF$^+$ DLP neurons majorly contribute to development on NR, and are activated by NR

In the larval CNS, Crz is expressed in 3 pairs of DLPs (Dorso Lateral Peptidergic neurons) in the *pars lateralis* region of the brain lobes, 1 pair of neurons in dorso-medial region and 8 pairs of interneurons in the VG (ventral ganglion) [30]. Other than the dorso-medial neurons, the *Crz-GAL4* used in this study recapitulates the known expression pattern for Crz. (Fig. S2A, B; Cartoon: Fig. 2A). Additionally, adjacent to DLPs, low expression of *Crz-GAL4* was observed in 3-4 neurons that do not express Crz (Fig. S2A and Fig. S2C). As mentioned previously, Crz$^+$ DLPs co-express sNPF [24]. In terms of neuronal architecture, the DLP neurons have two major branches: the anterior branch culminates in a dense nest of neurites at the ring gland (RG), while the posterior branch terminates in the subesophageal zone (SEZ). The VG neurons form a network amongst themselves to ultimately give rise to two parallel bundles that travel anteriorly, and end in the brain lobes. To visualize the overall distribution of NPs in the Crz neurons, we ectopically expressed a rat neuropeptide coupled to GFP (ANF::GFP), a popular tool used to track NP transport and release in *Drosophila* [31] (Fig. S2D). Firstly, within the DLPs, like Crz::mcherry (Fig. S2A), ANF::GPF was either in the cell bodies or RG projections, but not in the projections terminating at the subesophageal zone (Fig. S2D), suggesting selective NP transport to the RG, which is a major neurohaemal site for systemic release of neuropeptides. Secondly, ANF::GFP intensity was higher in the cell bodies of the DLPs than VG neurons (Fig. S2D).

The close proximity of the terminal projections of the Crz$^+$ VG neurons and the anterior branch of the Crz$^+$ DLP neurons in the brain lobe suggested possible neuromodulation between the two sets of neurons. Therefore, we undertook experiments to distinguish the contribution of DLPs vs VG localized Crz neurons, to the development in

NR media. First, we utilized *tshGAL80* to restrict *Crz-GAL4* expression to the DLPs (Fig. S2E). The level of pupariation under NR conditions observed with restricted expression of $dSTIM^{IR}$ (Fig. 2B; Mean: 51%±4.2) was similar to that seen with full expression (Fig. 1B; Mean: 40.7%±13.3), suggesting a major contribution of the DLP neurons to the NR phenotype. Furthermore, $sNPF>Crz^{IR}$ larvae have levels of pupariation of NR larvae (Fig. S2F; Mean: 30.9%±7.8) similar to $Crz>Crz^{IR}$ NR larvae (Fig. 1C; Mean: 33.8%±5.9). Because *sNPF-GAL4* marks only the Crz^{+} DLP neurons and not the Crz^{+} VG neurons (Fig. S1C), this too suggests a major role for the Crz^{+} DLP neurons.

Requirement of SOCE in Crz neurons for pupariation on NR (Fig. 1C) suggested that these neurons experience elevated cytosolic Ca^{2+} in NR conditions and are therefore, stimulated by chronic starvation. To test this, the UV light-activated genetically encoded calcium sensor, CaMPARI [32], was utilised. The sensor fluoresces in the GFP range (F_{488}) and is converted irreversibly to fluoresce in the RFP range (F_{561}), when exposed to UV light and in the presence of Ca^{2+}. The level of conversion positively titrates with Ca^{2+} concentrations. Larva expressing CaMPARI in Crz^{+} neurons were placed in either normal or NR media for 24 hours (24h NR). Whole larvae were immobilized, and exposed to UV light for 2mins. Control larva were subject to the same treatment but, without being exposed to UV light (Fig. 2C,D; no UV). Detection of F_{561} in the fed state suggests that these neurons are active even under normal food conditions (Fig. 2C,D). Notably, after 24 hours on NR media, chronic starvation caused a ~2-fold increase in average levels F_{561} and therefore, of neuronal activation (Fig. 2D). F_{561}/F_{488} ratios did not appear to change in the VG neurons (Fig. S2G,H). While there is a possibility that VG neurons do not exhibit higher F_{561} because of insufficient penetration of UV light, the CaMPARI results together with the genetic

209 experiments (Fig. 2B, S2F), formed the basis for selecting the DLP neurons for further

210 analysis on how dSTIM affects Crz and sNPF.

211

Figure 2

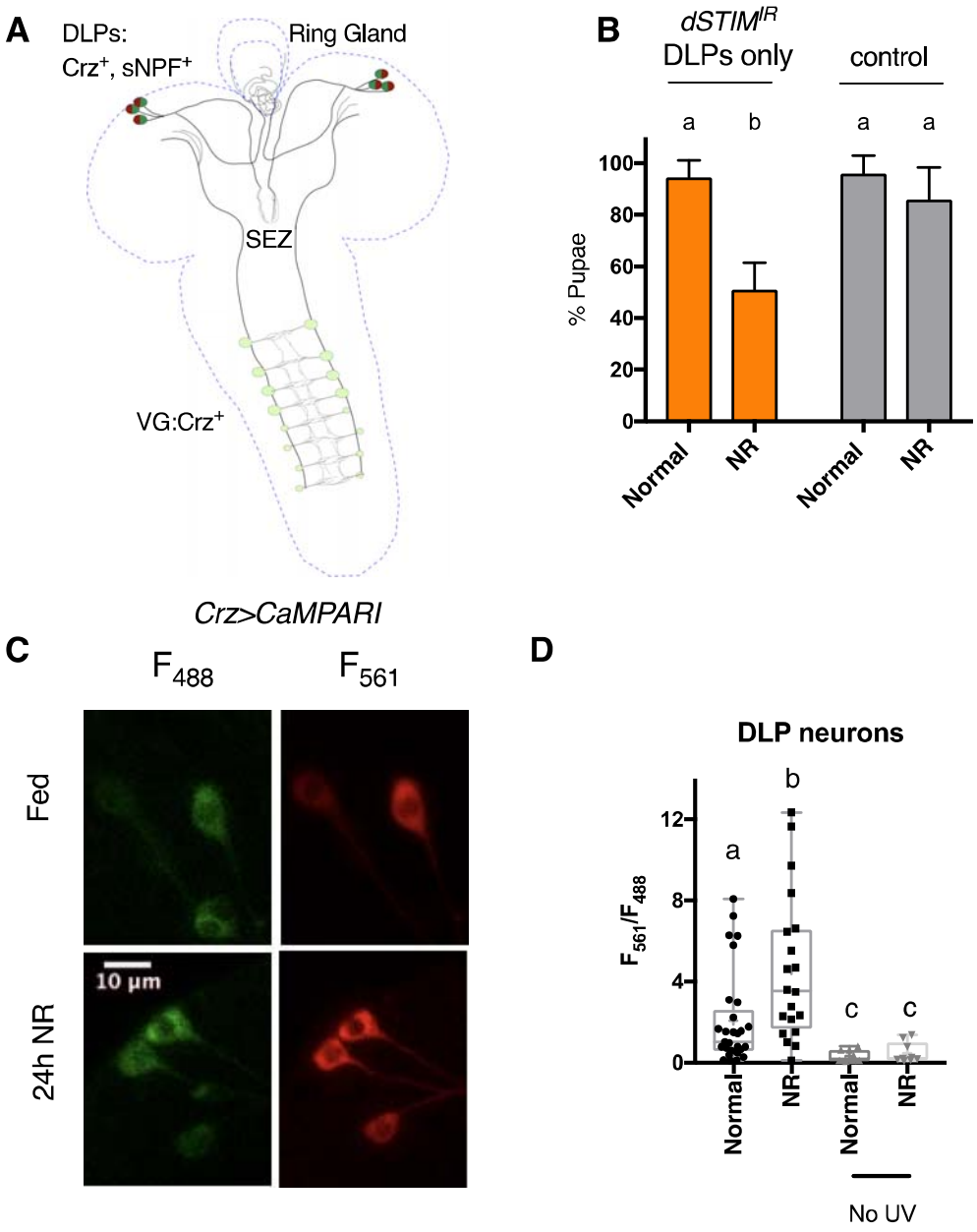

212

213 **Fig. 2 Crz$^+$ and sNPF$^+$ DLPs are required for development on NR media and activated by**

214 **NR (A)** Cartoon of Crz$^+$ and sNPF$^+$ neurons in the larval CNS marked by *Crz-GAL4*. DLP:

dorso lateral peptidergic; VG: Ventral Ganglion; SEZ: Subesophageal zone **(B)** % Pupae when *dSTIM* is selectively down-regulated only in Crz^{+} and $sNPF^{+}$ DLPs, by using the *tsh-Gal80* transgene and in the presence of *dicer2*. Control: *tshGal80/+;dSTIM^{IR}/+* . Data represents mean ± SEM **(C)** Representative image. Expression of the UV-activated Ca^{2+} indicator, CaMPARI in Crz^{+} and $sNPF^{+}$ DLPs, in larvae on 24 hours of normal (Fed) or NR media (24h NR). Fluorescence at 561nm (F_{561}) reflects Ca^{2+} levels, while at 488nm (F_{488}) reflects levels of the indicator CaMPARI. **(D)** Quantification of Ca^{2+} levels as reported by $F_{561/488}$ ratio in DLPs in larvae on 24 hours of normal or NR media, in the presence and absence of UV-stimulation. N>7 larvae for UV-stimulated; N=3 for No UV stimulation. Bars with the same alphabet represent statistically indistinguishable groups. Two-way ANOVA with Sidak multi comparison test $p<0.05$ for (B). Mann-Whitney Test for (D). See also Figure Supplement 2.

227 **_dSTIM_ regulates NP synthesis and release in Crz neurons**

228 Crz peptide levels were measured in DLP neurons by staining larval brains with an
229 antiserum raised against the mature Crz peptide sequence [33]. Two locations on the DLP
230 neurons were chosen for measurement: neuronal cell body/soma and neurite projections
231 on the RG. In control DLP neurons, 24 hrs of NR caused average levels of Crz levels to
232 increase, in both locations (Fig. 3A, S3A,B). In comparison, DLP neurons expressing $dSTIM^{IR}$
233 displayed increased Crz peptide levels on normal food itself, and this remained unaltered
234 upon NR, for both locations (Fig. 3A, S3B, C). sNPF levels could not be similarly measured
235 by immunofluorescence because sNPF is expressed in many neurons close to the DLPs (Fig.
236 S1C), making measurements specifically from the DLP soma difficult to quantify. Instead,
237 semi-quantitative, direct, mass spectrometric profiling of dissected RGs was employed.
238 This technique can measure peptide levels relative to stable isotopic standards at single
239 neurohaemal release sites [34]. As Crz levels between the cell bodies and projections
240 correlated, and Crz^{+} DLPs are the sole contributors of sNPF on the RG [24], this technique
241 allowed us to infer sNPF levels in DLPs. In controls, 24hrs of NR, increased the average level
242 of sNPF ~5-fold on the RG (Fig. 3C). In comparison, RG preparations from larvae where
243 DLPs express $dSTIM^{IR}$, displayed increased sNPF levels on normal food itself, and this
244 remained unaltered upon NR (Fig. 3C). Although Crz was detected in the RG preparations, it
245 was of much lower intensity. Average Crz levels increased with NR in the control, and in
246 $dSTIM^{IR}$ condition, but statistically higher levels of Crz were seen only in the NR, $dSTIM^{IR}$
247 condition (Fig. S3E). Nonetheless, broad agreement in trends, between Crz using
248 immunofluorescence and sNPF using MALDI-MS, suggest that the two peptides are
249 similarly regulated by NR and *dSTIM*. This is consistent with genetic experiments which

showed that over-expression of *dSTIM* can rescue loss of both, sNPF as well as Crz (Fig. 1C,D).

Thus, increased activation of DLP neurons by NR (Fig. 2D), appears to result in peptide accumulation. Loss of *dSTIM* increases peptide levels on normal food, and prevents an increase in peptide levels upon NR.

As an ER-Ca^{2+} sensor, *dSTIM* may potentially regulate several cellular processes that would affect NPs such as their synthesis, processing, trafficking and/or release. As $STIM^{IR}$ increased peptide levels in the cell body as well as neurite projections on the RG, a major trafficking defect was unlikely (Fig. 3A vs S3B,C). This does not rule out a role for *dSTIM* in dense-core vesicle trafficking, but merely indicates that trafficking of Crz is not observably disrupted by $STIM^{IR}$. We therefore proceeded to examine systemic and cellular phenotypes when molecules known to reduce overall NP synthesis (InR^{IR}; Insulin Receptor) [35], peptide processing ($amon^{IR}$) [25], and vesicle exocytosis (Ral^{DN}) [17] were expressed in Crz neurons. All three perturbations caused a pupariation defect on NR media (Fig. 3D). However, despite similar systemic outcomes, $amon^{IR}$, which reduces the prohormone convertase required for peptide maturation, reduced Crz levels (Fig. 3E). Because this is not seen with $STIM^{IR}$, a role for dSTIM in peptide processing was not pursued further.

Expression of InR^{IR} caused a modest increase in Crz peptide levels in DLP neurons in the fed state and peptide levels did not increase as in the control, in NR media (Fig. 3F). InR is a global protein synthesis regulator, and its expression scales $DIMM^{+}$ NE cell size, with functional consequences [35]. As the Crz^{+} DLPs are $DIMM^{+}$ [36], we expected InR^{IR} to reduce, not increase peptide levels. A potential explanation for this observation is that Crz peptide levels are under feedback regulation, which was substantiated when we examined how Crz transcript and peptide levels are connected. Similarities between InR^{IR} and $STIM^{IR}$

274 phenotypes, coupled with a previous observation that IP_3R, another SOCE component,
275 positively regulates protein synthesis in *Drosophila* neuroendocrine cells [22], prompted us
276 to test if *dSTIM* too regulates protein synthesis in general. We ectopically expressed a
277 physiologically irrelevant neuropeptide construct (ANF::GFP), that yields a processed
278 peptide in *Drosophila* neurons [31]. ANF::GFP levels in control and $dSTIM^{IR}$ DLP neurons
279 were similar (Fig. S3E), suggesting that dSTIM does not have generic effects on peptide
280 synthesis. Instead, its effect on Crz and sNPF synthesis may be specific. The lack of Crz
281 elevation upon NR, in DLP neurons where InR^{IR} is expressed, leads to the speculation that
282 InR signalling is required for the up-regulation of protein synthesis needed for increased
283 peptide synthesis, processing and packaging during NR.
284 We previously found that *Ral* expression lies downstream of dSTIM-mediated SOCE
285 in *Drosophila* pupal brains [37], and in dopaminergic neurons, over-expression of Ral^{DN}
286 reduces secretion of ANF::GFP [17]. These previous data, coupled with the observation that
287 Ral^{DN} and $dSTIM^{IR}$ show similarly high Crz levels in the fed state, suggest that *dSTIM* affects
288 vesicle secretion through regulation of *Ral* expression. To independently validate if vesicle
289 release is important in Crz neurons, we over-expressed a temperature sensitive dynamin
290 mutant ($Shibire^{ts}$) also shown to reduce NP release [38] and tetanus toxin (*TNT*) shown to
291 prevent release of eclosion hormone, a neuropeptide [39]. Both manipulations caused a
292 pupariation defect on NR (Fig. S3F). It is unclear why Ral^{DN} causes Crz levels to decrease
293 upon NR. In *Drosophila* pacemaker neurons, *Ral* has been shown to bias the sensitivity of a
294 neuropeptide receptor, the Pigment Dispensing Factor Receptor [40]. Perhaps, functions
295 distinct from *Ral*'s contribution to vesicle exocytosis contribute to this observation.
296 Nonetheless, the lack of increase in Crz levels in DLP neurons upon NR, when InR^{IR} and
297 Ral^{DN} are expressed, assumes significance in the context of pupariation of NR larvae.

298 Control larvae subject to 24hrs of NR, display increased Crz (Fig. 3A) and sNPF (Fig. 3C)
299 levels, and then proceed to successfully complete development to pupae (Fig. 1C).
300 Whereas, in d*STIM*^{IR}, *InR*^{IR} and *Ral*^{DN} conditions, on NR, neither do DLPs display increased
301 Crz levels (Fig. 3A, 3F), nor do all larvae pupariate (Fig. 1B, 1C, 3D). Thus, an increase in
302 peptide levels on NR correlates with larval ability to pupariate on NR. Taken in context with
303 increased neuronal activation during NR (Fig. 2D), and evidence that functional vesicle
304 exocytosis (Fig. 3D, S3F) as well as adequate peptide production (Fig. 3D) is required for
305 survival on NR, these data suggest that increased production and release of Crz and sNPF
306 during NR, is required for NR larvae to successfully complete development.
307 To prove that Crz and sNPF are released during NR, the ideal experiment would be
308 to measure levels of secreted NPs. But small size (8-10 amino acids), low hemolymph titres
309 and high complexity of hemolymph, make peptide measurements by biochemical means
310 highly challenging in *Drosophila*. Moreover, NPs exhibit endocrine as well as paracrine
311 signalling [41]; and the latter will not be reflected in hemolymph measurements.
312 Fortunately, in the Crz signalling system there is feedback compensation between secreted
313 Crz and Corazonin receptor (*CrzR*) mRNA levels, providing a means to gauge secreted Crz
314 levels indirectly. In adults, expression of *Crz*^{IR} in Crz neurons, increased levels of *CrzR* on the
315 fat body [42]. We thus tested if *CrzR*, which in larvae appears to be expressed in the salivary
316 glands and CNS [43], was subject to similar feedback. In larval brains, reducing Crz, using
317 two different *Crz*^{IR} strains, not only caused a reduction in *Crz* mRNA levels (Fig. 3G), but also
318 a concomitant increase in *CrzR* mRNA levels (Fig. 3H). Conversely, reducing CrzR levels
319 (*CrzR*^{IR}) in the larval CNS, results in up-regulation of *Crz* mRNA (Fig. S3G). This confirmed
320 the existence of feedback in the Crz signalling system, and the use of neuronal *CrzR*
321 transcript levels as a measure of secreted Crz levels. In line with this inference, we observed

an up-regulation of *CrzR* mRNA in larval brains where Crz neurons are expressing either *InR*^{IR} or *amon*^{IR} or *Ral*^{DN} (Fig. 3I). Therefore, the observation that in the *STIM*^{IR} condition *CrzR* mRNA levels are high (Fig. 3I), supports the idea that dSTIM function is necessary for the secretion of optimal levels of Crz.

Because dSTIM-mediated SOCE is known to induce changes in gene expression [37], we probed if *Crz* expression is sensitive to NR and *dSTIM*. In the control, NR did not change *Crz* mRNA levels (Fig. 3J), suggesting that a post-transcriptional mechanism is responsible for increasing Crz peptide levels upon NR (Fig. 3A,S3B,C). In the *STIM*^{IR} condition, *Crz* transcript levels were up-regulated on normal food conditions (Fed) and no further increase was observed upon NR (Fig. 3J). The straightforward explanation for high Crz peptide levels in *STIM*^{IR} condition could therefore be attributed to higher gene expression of *Crz*. However, data from other perturbations in Crz neurons suggested that a linear interpretation between *Crz* mRNA and peptide levels cannot not be made. When *Crz*^{IR} is expressed, *Crz* mRNA is reduced (Fig. 3G), but peptide levels are elevated (Fig. S3I); whereas, when *amon*^{IR} is expressed, *Crz* mRNA is increased (Fig. S3H), but peptide levels are decreased (Fig. 3E). Meanwhile, in three conditions, *Crz* mRNA as well as peptide levels are higher than controls: *CrzR*^{IR} (Fig. S3G vs S3I), *InR*^{IR} (Fig. S3H vs Fig. 3F) and *Ral*^{DN} (Fig. S3H vs Fig 3F). Note also that both higher (d*STIM*^{IR}, *InR*^{IR}, *Ral*^{DN}) or lower (*amon*^{IR}) Crz peptide levels in DLP cell bodies, result in reduced systemic Crz signalling (*CrzR* mRNA levels; Fig. 3I). These data indicate that Crz transcription, translation and release are independently regulated. A simple explanation for elevated levels of *Crz* transcript as well as peptide levels in *STIM*^{IR} is therefore, feedback compensation. Moreover, there is no change in Crz mRNA upon 24hrs of NR, when *STIM*^{IR} is expressed (Fig. 3J). Together, this argues against a direct role for *dSTIM* in regulating *Crz* gene expression.

In summation, these data have been inferred as follows: on normal food, partial loss of *dSTIM* reduces systemic Crz signalling, indicating a requirement for *dSTIM* in Crz secretion. On NR media, Crz^{+} DLPs are stimulated to increase peptide synthesis and release, in order for NR larvae to complete development. Peptide up-regulation upon NR is abrogated when *dSTIM* is reduced. These add up to suggest that *dSTIM* compromises NE cell function in a manner that affects peptide synthesis and release, with functional consequences for survival on NR.

Figure 3

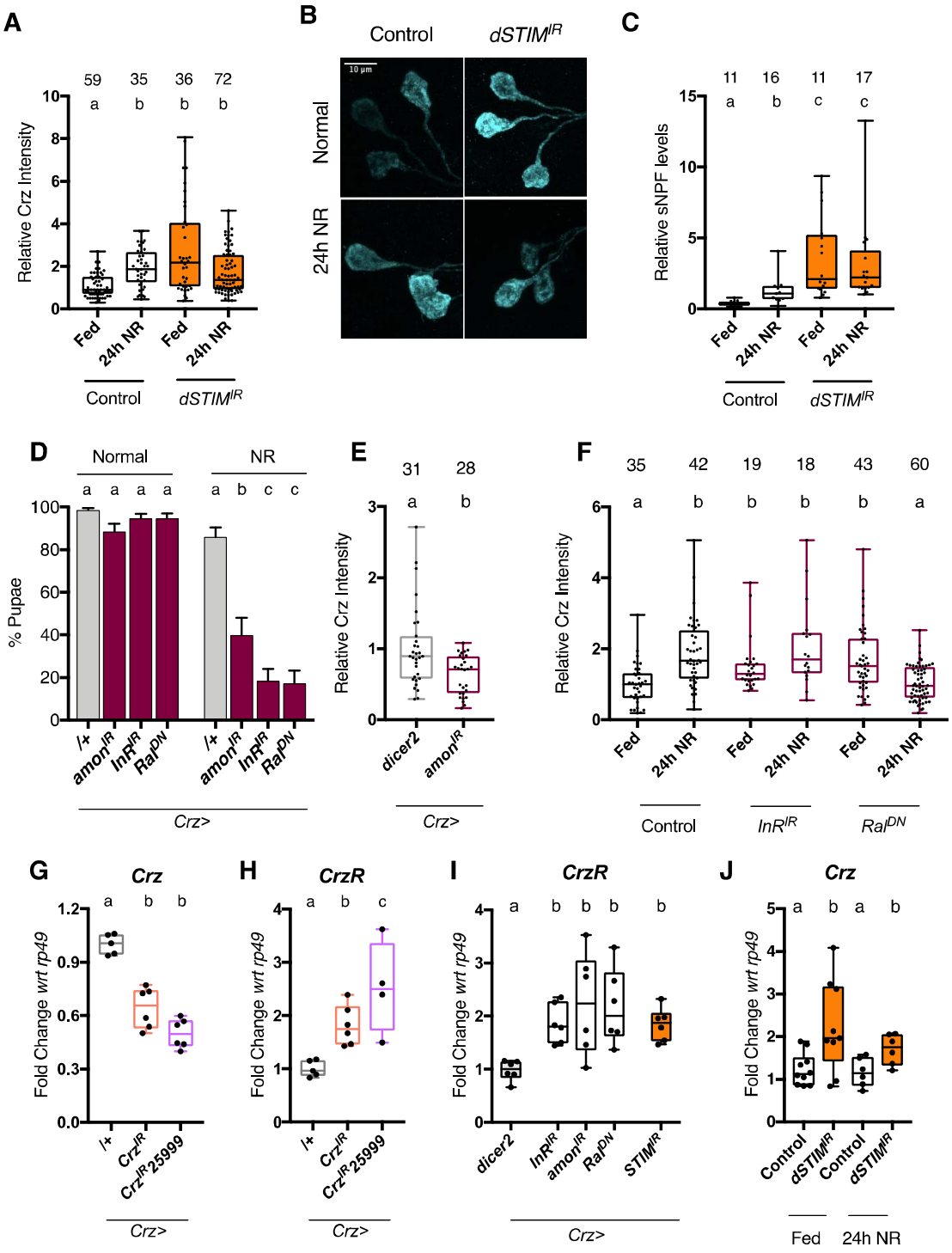

Fig 3. *dSTIM* regulates Crz and sNPF levels. Larvae were subjected to 24 hours of normal (fed) or nutrient restricted (NR) media. Crz levels were measured in DLP neurons by

356 immunofluorescence on larval brains. All manipulations were performed using the *Crz-*
357 *GAL4* driver **(A)** Relative levels of Crz peptide in DLP neuron cell bodies, Control=*crz>dicer2*
358 . $dSTIM^{IR}$=*crz*> $dSTIM^{IR}$,*dicer2*. Number of cells measured shown atop bars. N>12 brains **(B)**
359 Representative images for cell bodies measured in (A). **(C)** Relative levels of total sNPF
360 peptides measured on dissected ring glands (N atop bars) and quantified using MALDI-MS.
361 Externally added heavy standard (Hug-PK*) was used to normalise peptide levels between
362 samples. **(D)** % Pupae on normal or NR media, upon reduced peptide processing
363 ($amon^{IR}$,*dicer2*) protein synthesis (Insulin receptor; InR^{IR}) or vesicle exocytosis (dominant-
364 negative *Ral*; Ral^{DN}) in Crz^{+} neurons. Data represents mean ± SEM **(E)** Relative levels of Crz
365 upon expression of $amon^{IR}$ and *dicer2*. N>10 brains. **(F)** Relative levels of Crz upon indicated
366 cellular perturbation of Crz^{+} neurons. N≥6 brains. control: *Crz-GAL4*/+. **(G)** *Crz* mRNA levels
367 from larval brains when *Crz* is reduced by two different RNAi lines. N ≥ 5. (**H)** Corazonin
368 receptor (*CrzR)* mRNA levels from larval brains with reduced *Crz*. N ≥ 4. **(I)** *CrzR* mRNA
369 levels from larval brains expressing indicated cellular perturbations in Crz neurons. N ≥ 6 **(J)**
370 *Crz* mRNA levels from larval brains. Control=*crz>dicer2* . $dSTIM^{IR}$=*crz*> $dSTIM^{IR}$,*dicer2* N ≥ 6.
371 Bars with the same alphabet represent statistically indistinguishable groups. Kruskal-Wallis
372 Test with Dunn's multicomparison correction $p<0.05$ for (A), (C), (F). Mann-Whitney Test
373 for (E). Two-way ANOVA with Sidak's multi comparison test $p<0.05$ for (D), (J). One-way
374 ANOVA with Tukey multi comparison test $p<0.05$ for (G), (H), (I). See also Figure
375 Supplement 3.

Systemic and cellular phenotypes observed with reduced *dSTIM* in Crz neurons can be rescued by increasing synthesis and release of peptides

To validate a role for dSTIM in peptide synthesis and release, we tested genetic perturbations that can compensate for this deficiency, to rescue developmental and cellular phenotypes associated with $dSTIM^{IR}$ expression in Crz neurons. In the case of NPs, genetic over-expression may not translate to enhanced release, as proteins involved in NP processing as well as the regulated secretory pathway would need to be up-regulated. Furthermore, regulatory feedback from peptides to their transcription may complicate over-expression, as seen for the Crz signalling system (Fig. S3I). To get around these issues, and because InR^{IR} phenocopied $STIM^{IR}$ (Fig. 3A,D,F,I, S3H), we opted to increase protein synthesis by over-expression of the Insulin receptor (*InR*). Cell size (Fig. S4A) as well as Crz levels (Fig. S4B,C) in DLP neurons scaled with *InR* over-expression, supporting the effectiveness of *InR*. To increase release, we over-expressed Ral^{WT} as *Ral* over-expression can compensate for vesicle release in dopaminergic neurons expressing $STIM^{IR}$ [17]. In Crz neurons with reduced *dSTIM*, over-expression of either *InR* or Ral^{WT} rescued pupariation on NR media (Fig. 4A); restored peptide up-regulation upon NR (Fig. 4A,B) and decreased *CrzR* mRNA back to control levels (Fig. 4D). Of note, over-expressing Ral^{WT} or *InR* by itself, in Crz neurons, did not alter *CrzR* mRNA levels (Fig. 4D), suggesting that neuronal activation, which happens on NR media (Fig. 2D) potentiates their activity.

To increase neuronal activity, we utilised the temperature and voltage-gated cation channel, TrpA1 [44]. Over-expression of *dTrpA1* and its activation by raising the temperature to 30°C for 24 hours, in the $dSTIM^{IR}$ background, rescued pupariation of NR larvae (Fig. 4E). It also restored the ability of DLP neurons to increase Crz levels upon NR

(Fig. 4F) and decreased levels of *CrzR* mRNA (Fig. 4G). In line with the feedback between *CrzR* mRNA levels and systemic Crz signaling, over-expression of *dTrpA1* alone in Crz neurons resulted in a decrease in *CrzR* mRNA levels (Fig. 4G), supporting the role for neuronal activation in secreting Crz. Interestingly, development to adulthood on NR, for $dSTIM^{IR}$ larvae, was also significantly increased upon over-expression of *InR* (Fig. S4E) and *TrpA1* (Fig. S4F), but not Ral^{WT} (Fig. S4E).

An optogenetic approach, utilizing the over-expression of Channelrhodopsin (ChR2-XXL), a light-sensitive cation channel, also rescued pupariation but not to the same extent (Fig. S4D). Poorer rescue with *ChR2-XXL* could be because sustained activation of this channel depress synaptic transmission and the channel is less conductive for Ca^{2+} compared to TrpA1 [45]. Similar genetic manipulation, with TrpA1 and Chr2-XXL, in a hypomorphic IP_3R mutant ($itpr^{ku}$) resulted in a small but significant rescue of $itpr^{ku}$ pupariation on NR media (Fig. S4G,H).

Together, these results strongly suggested that defects arising from dysregulated intracellular Ca^{2+} signalling, may be overcome by increasing vesicle exocytosis (Ral^{WT}, *TrpA1, ChR2-XXL rescue*) or protein synthesis (*InR* rescue). Importantly, the rescues observed with *InR*, Ral^{WT} and *dTrpA1* are effective at the molecular (*CrzR* levels), cellular (Crz peptide levels upon NR) as well as systemic (NR larvae) level.

Figure 4

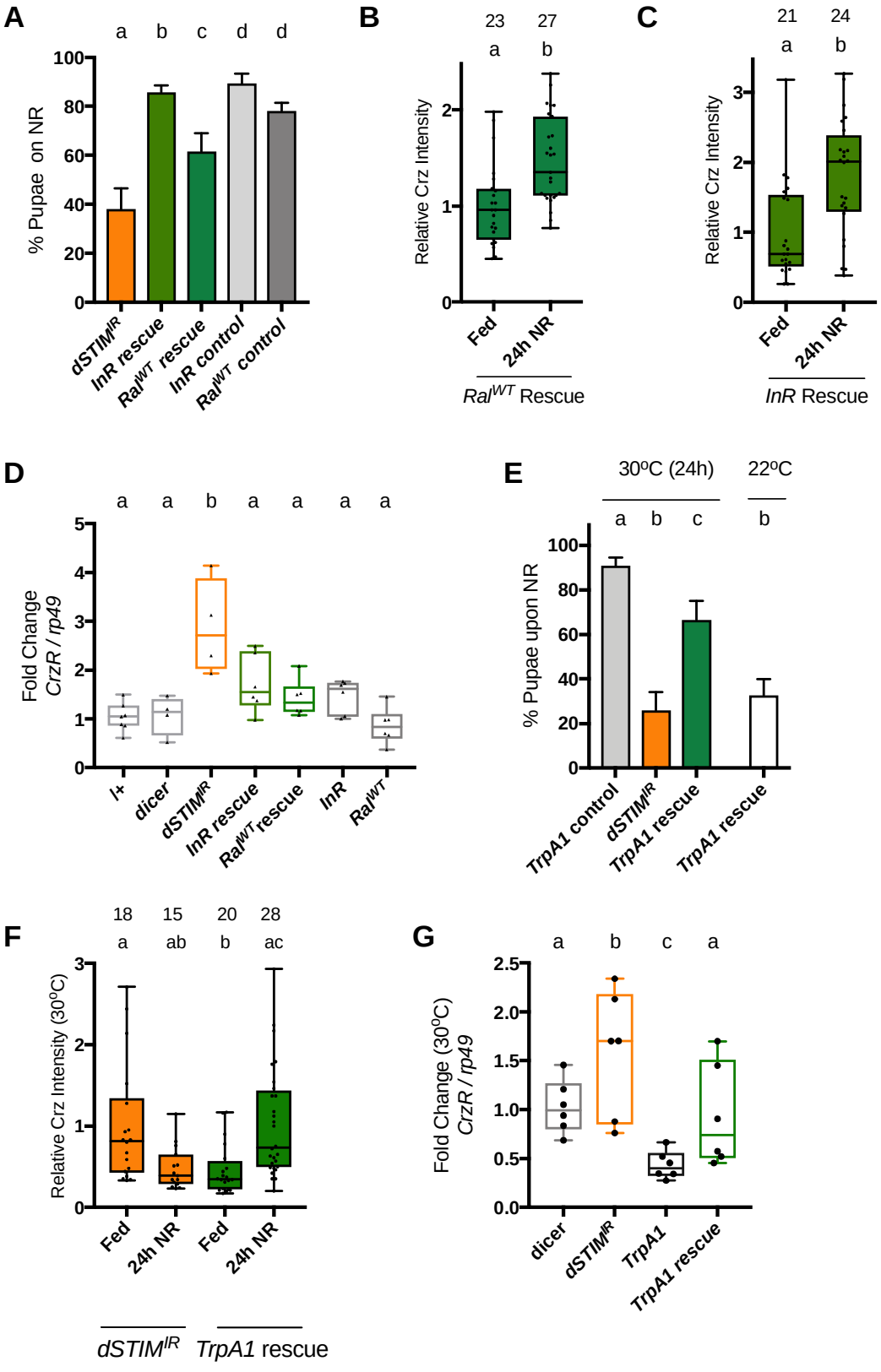

419

Fig 4. Systemic and cellular phenotypes caused by partial loss of dSTIM in Crz neurons, can be rescued by increasing peptide synthesis or release. **(A)** % Pupae upon expression of Insulin receptor (*InR*) or Ral (Ral^{WT}) in Crz neurons expressing $dSTIM^{IR}$. Genotypes: $dSTIM^{IR}$ = *crz>*$dSTIM^{IR}$. InR rescue=*Crz>InR,*$dSTIM^{IR}$,*dicer2*. Ral^{WT}rescue=*Crz>* Ral^{WT}, $dSTIM^{IR}$,*dicer2*. *InR* control: *dicer2;InR/+;* $dSTIM^{IR}$ /+;. Ral^{WT} control: Ral^{WT}/+; $dSTIM^{IR}$ /+. Data represents mean ± SEM. **(B)** Ral^{WT}rescue or **(C)** InR rescue larvae were transferred to normal (Fed) or NR media for 24 hours. Crz immunofluorescence levels in DLP neurons were measured. Number of cells measured shown atop bars. N>7 brains **(D)** *Crz* receptor *(CrzR)* mRNA levels in larval brains expressing various molecules in Crz neurons. InR=*Crz>InR*. Ral^{WT}=*Crz>*Ral^{WT}. N≥4. **(E)** % Pupae upon expression of TrpA1 in Crz neurons expressing $dSTIM^{IR}$. TrpA1 control: *dicer2;TrpA1/+;* $dSTIM^{IR}$ /+; TrpA1 rescue: *Crz>TrpA1,* $dSTIM^{IR}$,*dicer2*. Larvae were reared at 25°C, at 88h±3h AEL age transferred to NR media and incubated either at 30°C or 22°C for 24 hours, and returned to 25°C thereafter. Data represents mean ± SEM. **(F)** Crz levels in DLP neurons upon 24 hrs of NR or normal food (Fed) at 30°C for indicated genotypes. N > 5 brains. **(G)** *Crz* receptor *(CrzR)* transcript levels in larval brains expressing various molecules in Crz^{+} neurons, when larvae are reared at 30°C. TrpA1: *Crz>TrpA1*. N=6. one-way ANOVA with a post hoc Tukey's test p<0.05 for (A), (D), (E), (G). Mann-Whitney test for (B), (C). Kruskal-Wallis Test with Dunn's multi-comparison correction p<0.05 for (F). See also Figure Supplement 4.

Discussion

This study employed an *in vivo* approach coupled to a functional outcome, in order to broaden our understanding of how STIM regulates neuropeptides. A role for dSTIM-mediated SOCE in *Drosophila* neuroendocrine cells for survival on NR was previously established [22]. The previous study offered the opportunity to identify SOCE-regulated peptides, produced in these neuroendocrine cells, that could be investigated in a physiologically relevant context.

In *Drosophila*, both Crz and sNPF have previously been attributed roles in many different behaviours. Crz has roles in adult metabolism and stress responses [42,46–48], sperm transfer and copulation [49], and regulation of ethanol sedation [50,51]. While, sNPF has been implicated in various processes including insulin regulation (Kapan et al., 2012; Lee et al., 2008) circadian behaviour [53], sleeping [54,55] and feeding [27]. Thus, the identification of Crz and sNPF in coping with nutritional stress is perhaps not surprising, but a role for them in coordinating the larval to pupal transition under NR is novel.

A role for Crz in conveying nutritional status information was originally proposed by Jan Veenstra [56], which this study now supports. In larvae, Crz^{+} DLPs are known to play a role in sugar sensing [57] and in adults, they express the fructose receptor Gr43a [58]. Additionally, they express receptors for neuropeptides DH31 [59], DH44 [59] and AstA [56], which are made in the gut as well as larval CNS. Together, these observations and our study are strongly indicative of a role for Crz^{+} DLPs in directly or indirectly sensing nutrients, with a functional role in larval survival and development in nutrient restricted conditions.

Several neuropeptides and their associated signalling systems are evolutionarily conserved [11,12]. The similarities between Crz and GnRH (gonadotrophin-releasing hormone), and sNPF and PrRP (Prolactin-releasing peptide), at the structural [11],

464 developmental [60] and receptor level therefore, is intriguing. Structural similarity of
465 course does not imply functional conservation, but notably, like sNPF, PrRP has roles in
466 stress response and appetite regulation [61]. This leads to the conjecture that GnRH and
467 PrRP might play a role in mammalian development during nutrient restriction.

468 dSTIM regulates Crz and sNPF at the levels of peptide release and likely, peptide
469 synthesis upon NR. We speculate that neuroendocrine cells can use these functions of
470 STIM, to fine tune the amount and timing of peptide release, especially under chronic
471 stimulation (such as 24hrs NR), which requires peptide release over a longer timeframe.
472 Temporal regulation of peptide release by dSTIM may also be important in neuroendocrine
473 cells that co-express peptides with multifunctional roles, as is the case for Crz and sNPF. It
474 is conceivable that such different functional outcomes may require distinct bouts of NP
475 release, varying from fast quantile release to slow secretion [62]. As elevation in cytosolic
476 Ca^{2+} drives NP vesicle release, neurons utilise various combinations of Ca^{2+} influx
477 mechanisms to tune NP release. For example, in *Drosophila* neuromuscular junction,
478 octopamine elicits NP release by a combination of cAMP signalling and ER-store Ca^{2+}, and
479 the release is independent of activity-dependent Ca^{2+} influx [63]. In the mammalian dorsal
480 root ganglion, VGCC activation causes a fast and complete release of NP vesicles, while
481 activation of TRPV1 causes a pulsed and prolonged release [64]. dSTIM-mediated SOCE
482 adds to the repertoire of mechanisms that can regulate cytosolic Ca^{2+} levels and therefore,
483 vesicle release. This has already been shown for *Drosophila* dopaminergic neurons [17] and
484 this study extends the scope of release to peptides. Notably, dSTIM regulates exocytosis
485 via Ral in neuroendocrine cells, like in dopaminergic neurons.

486 In *Drosophila* larval Crz^{+} DLPs, dSTIM appears to have a role in both fed, as well as
487 NR conditions. On normal food, not only do Crz^{+} DLPs exhibit small but significant levels of

488 neuronal activity (Fig. 2D) but also, loss of dSTIM in these neurons reduced Crz signalling
489 (Fig. 3I). Thus, dSTIM regulates Ca^{2+} dynamics and therefore, neuroendocrine activity,
490 under basal as well as stimulated conditions. This is consistent with observations that basal
491 SOCE contributes to spinogenesis, ER-Ca^{2+} dynamics as well as transcription [65].
492 However, in our case, this regulation appears to have functional significance only in NR
493 conditions as pupariation of larvae, with reduced levels of *dSTIM* in Crz^{+} neurons, is not
494 affected on normal food (Fig. 1B). In a broader context, STIM is a critical regulator of
495 cellular Ca^{2+} homeostasis as well as SOCE, and a role for it in the hypothalamus has been
496 poorly explored. Because STIM is highly conserved across the metazoan phyla, our study
497 predicts a role for STIM and STIM-mediated SOCE in peptidergic neurons of the
498 hypothalamus. There is growing evidence that SOCE is dysregulated in neurodegenerative
499 diseases [66]. In neurons derived from mouse models of familial Alzheimer's' disease [67]
500 and early onset Parkinson's [65], reduced SOCE has been reported. How genetic mutations
501 responsible for these diseases manifest in neuroendocrine cells is unclear. If they were to
502 also reduce SOCE in peptidergic neurons, it's possible that physiological and behavioural
503 symptoms associated with these diseases, may in part stem from compromised SOCE-
504 mediated NP synthesis and release.

505 **Material and Methods**

506 **Fly Husbandry**

507 Flies were grown at 25°C in 12h:12h L:D cycle. Normal food: (1L recipe: 80g corn flour,
508 20g Glucose, 40g Sugar, 15g Yeast Extract, 4mL propionic acid, *p*-hydroxybenzoic
509 acid methyl ester in ethanol 5mL, 5mL ortho butyric acid) For nutritional stress assay,
510 flies were allowed to lay eggs for 6 hours on normal food. After 88hours, larvae were

collected and transferred to either normal or NR (100mM Sucrose) food. Pupae and adults were scored after 10 days of observation.

Fly strains.

Canton S was used as the wild type (+) control.

The following strains were obtained from Bloomington Drosophila Stock Centre: *AKH-GAL4* (25684), *Crz-GAL4* (51976), *DSK-GAL4* (51981), *sNPF-GAL4* (51981), *UAS-Crz^{IR}*25999 (25999), *UAS-dicer2* (24651), *UAS-TeTxLc* (28837), *UAS-TeTxLc-IMP* (28838), *UAS-CaMPARI* (58761), *UAS-GFP^{nls}* (4776), *UAS-mRFP* (32218), *UAS-TrpA1* (26263), *UAS-InR* (8248), *UAS-amon^{IR}* (28583), *UAS-Ral^{DN}* (32094)

The following strains were obtained from Drosophila Genetic Resource Center, Kyoto: *sNPF-GAL4* (113901)

The following were from Vienna Drosophila Research Centre stock collection: *UAS-IP$_3$R^{IR}* (106982), *UAS-STIM^{IR}* (47073), *UAS-Crz^{IR}* (30670), *UAS-InR^{IR}*(999)

The following was from Exelixis at Harvard Medical School: *sNPF^{00448}* (c00448)

The following were kind gifts: *AstA^{1}-GAL4* (David Anderson), *dILP2-GAL4* (Eric Rulifson), *hug-GAL4* (Michael Pankratz), *NPF-GAL4* (Ping Shen), *UAS-sNPR^{IR}* (Kweon Yu), Crz::mCherry (Gábor Juhász), *UAS-hid::UAS-rpr* (Tina Mukherjee), *UAS-Shibire^{ts}* (Toshihiro Kitamoto), *tsh-GAL80* (Julie Simpson), *UAS-preproANF::GFP* (Edwin Levitan), *UAS-ChR2XXL* (Robert Kittel and Georg Nagel)

The following were previously generated in our laboratory: *itpr^{ka1091}*, *itpr^{ug3}*,*UAS-Orai^{E180A}*, UAS-*itpr^{+}*,*UAS-Stim, UAS-Ral^{WT}*

Larval Feeding

Ten 3rd instar larvae were collected and placed on cotton wool soaked with solution of 4.5% dissolved yeast granules and 0.5% Erioglaucine (Sigma, 861146). Controls contained no

dye. Feeding was allowed for 2 hours at 25°C. 5 larvae per tube were crushed in 100µL of double distilled water. Solution was spun at 14000 rpm for 15 minutes and 50µL was withdrawn for absorbance measurement at 625nm in a 96-well plate. 5µL was used to measure protein content using the Pierce BCA Protein Assay kit (#23227).

qRT-PCR

RNA was isolated from 12-15 larval brains at the specified time points using Trizol. cDNA synthesis was carried out as described [26]. All mRNA levels are reported as fold change normalized to *rp49*. Primer sequences:

rp49, F:CGGATCGATATGCTAAGCTGT, R:GCGCTTGTTCGATCCGTA.

Crz, F:TCCTTTAACGCCGCATCTCC, R:CGTTGGAGCTGCGATAGACA

CrzR, F:CTGTGCATCCTGTTTGGCAC, R:GGCCTTGTGTATCAGCCTCT

Measuring neuronal activation using *CaMPARI*

Early third instar larvae were transferred to either normal or NR food. After 24 hours, larvae were recovered and immobilized on double sided tape. UV light from a Hg-arc lamp was focused using the UV filter, on the larvae through a 10X objective on Olympus BX60, for 2 minutes. Larvae were them immediately dissected in ice-cold PBS, mounted in PBS and imaged using Olympus FV-3000 Confocal microscope using a 40X objective and high-sensitivity detectors. Microscope settings for laser intensity, PMT settings and magnification were kept identical for all measurements. Each experiment always had a no UV control, in which larvae were subject to immobilisation but not UV light. Fluorescence intensity was calculated for each cell body using Image J.

Immunofluorescent staining

For expression patterns, 3rd instar larval brains with RGs attached were dissected in ice-cold PBS and fixed in 3.7% formaldehyde at 4°C for 20mins. The samples were washed 4

559 times in PBS and mounted in 60% glycerol. Endogenous fluorescence was acquired on
560 Olympus FV-3000 using a 20X, 40X or 60X objective, and processed used ImageJ. For
561 samples requiring antibody staining brains were similarly processed and then subjected to
562 permeabilisation (0.3% Triton X-100 + PBS; PBSTx) for 15 mins, 4 hr blocking in 5% normal
563 goat serum in PBSTx at 4oC, followed by overnight incubation in primary antibody (1:1000
564 Chicken-GFP, Abcam: ab13970) and secondary with Alexa 488 or Alexa 594 (1:400; Abcam).
565 For corazonin (1:1000; raised in Rabbit; Jan Veenstra, University of Bordeaux), all the above
566 steps remained the step, except that dissected brains were fixed for 1hr at RT in 4% PFA
567 and the secondary was anti-rabbit Alexa 405 (1:300, Abcam). Cell bodies were outlined
568 manually and integrated density was used to calculate CTCF (Corrected Total Cell
569 Fluorescence). For all samples, a similar area was measured for background fluorescence.

570 **Direct peptide-profiling by MALDI-TOF MS**

571 Ring glands were dissected in cold HL3.1 and transferred to a MALDI plate as previously
572 described [68]. 0.2 µl of matrix (saturated solution of recrystallized α-cyano-4-
573 hydroxycinnamic acid in MeOH/EtOH/water 30/30/40% v/v/v) was added, containing 10 nM
574 of stable isotope-labeled HUG-pyrokinin (HUG-PK* (Ser–Val[d8]–Pro–Phe–Lys–Pro–Arg–
575 Leu–amide, Mw = 950.1 Da; Biosyntan, Berlin, Germany)) and 10 nM labeled
576 myosuppressin (MS* (Thr–Asp–Val[d8]–Asp–His–Val–Phe–Leu–Arg–Phe–amide, Mw =
577 1255.4 Da; Biosyntan) MALDI-TOF mass spectra were acquired in positive ion mode on a
578 4800 Plus MALDI TOF/TOF analyzer (MDS Sciex, Framingham, MA, USA) in a mass range
579 of 900-4000 Da and fixed laser intensity with 20 subspectra and 1000 shots per sample.
580 Data were analyzed with Data Explorer 4.10. Spectra were baseline corrected and de-
581 isotoped. The sum of the resulting relative intensities of the de-isotoped peaks was
582 calculated for the different ion adducts (H^+, Na^+, K^+) of each peptide as well as the labeled

583 peptides*. Then, the ratios sNPF/HUG-PK* and corazonin/MS* were calculated, using the
584 labeled peptide with the most similar molecular weight. For sNPF, all isoforms (1/2-short, 1-
585 long, -3 and -4) variants were totaled.

586 **Optogenetic and thermogenic experiments**

587 For thermogenetic (*dTrpA1*, *Shibire^{ts}*) experiments, larvae were matured to 88hours AEL at
588 25°C. After transfer to either NR or normal food, vials were placed at 22°C, 25°C or 30°C for
589 either 24 hours (*dTrpA1*) or till the end of observation time (*Shibire^{ts}*). For optogenetic
590 experiments (*Chr2-XXL*), larvae were matured to 88AEL in the dark. After transfer to either
591 NR or normal food, one set was placed in the dark while another was placed in an incubator
592 with regular white lights that were on continuously till the end of observation time.

593 **Author contributions**

594 M, C.W and G.H designed research; M performed research, except MALDI-MS which was
595 performed by C.W.; M, C.W and G.H. analysed data; M wrote the paper with inputs from
596 C.W. and G.H.

597 **Acknowledgments**

598 Supported by Wellcome Trust/ DBT India Alliance (Early Career Award #IA/E/12/1/500742 to
599 M) and NCBS core funding (GH). We thank Jan Veenstra for the Crz antibody and helpful
600 suggestions with immunostaining. Members of the Hasan lab for help with fly transfers,
601 critical comments and helpful discussions. Drosophila fly community (List in supplementary
602 information), BDSC, VDRC, NIG and DGRC for fly strains. NCBS Central Imaging and Flow
603 Facility, for imaging, and Jörg Kahnt (core facility for mass spectrometry and proteomics,
604 Max-Planck-Institute for Terrestrial Microbiology, Marburg) for access to the mass
605 spectrometer.

606 **Competing Interests**

All of the authors declare no financial and non-financial competing interests.

References

1. Prakriya M, Lewis RS. Store-Operated Calcium Channels. Physiol Rev. United States; 2015;95: 1383–1436. doi:10.1152/physrev.00020.2014
2. Putney JW, Steinckwich-Besançon N, Numaga-Tomita T, Davis FM, Desai PN, D'Agostin DM, et al. The functions of store-operated calcium channels. Biochim Biophys Acta - Mol Cell Res. 2017;1864: 900–906. doi:https://doi.org/10.1016/j.bbamcr.2016.11.028
3. Brini M, Cali T, Ottolini D, Carafoli E. Neuronal calcium signaling: function and dysfunction. Cell Mol Life Sci. Switzerland; 2014;71: 2787–2814. doi:10.1007/s00018-013-1550-7
4. Lalonde J, Saia G, Gill G. Store-operated calcium entry promotes the degradation of the transcription factor Sp4 in resting neurons. Sci Signal. United States; 2014;7: ra51. doi:10.1126/scisignal.2005242
5. Hartmann J, Karl RM, Alexander RPD, Adelsberger H, Brill MS, Ruhlmann C, et al. STIM1 controls neuronal Ca(2)(+) signaling, mGluR1-dependent synaptic transmission, and cerebellar motor behavior. Neuron. United States; 2014;82: 635–644. doi:10.1016/j.neuron.2014.03.027
6. Berna-Erro A, Braun A, Kraft R, Kleinschnitz C, Schuhmann MK, Stegner D, et al. STIM2 Regulates Capacitive Ca2+ Entry in Neurons and Plays a Key Role in Hypoxic Neuronal Cell Death. Sci Signal. 2009;2: ra67 LP-ra67. Available: http://stke.sciencemag.org/content/2/93/ra67.abstract
7. Sun S, Zhang H, Liu J, Popugaeva E, Xu N-J, Feske S, et al. Reduced synaptic STIM2 expression and impaired store-operated calcium entry cause destabilization of mature spines in mutant presenilin mice. Neuron. United States; 2014;82: 79–93. doi:10.1016/j.neuron.2014.02.019
8. Park CY, Shcheglovitov A, Dolmetsch R. The CRAC channel activator STIM1 binds and inhibits L-type voltage-gated calcium channels. Science. United States; 2010;330: 101–105. doi:10.1126/science.1191027
9. Wang Y, Deng X, Mancarella S, Hendron E, Eguchi S, Soboloff J, et al. The calcium store sensor, STIM1, reciprocally controls Orai and CaV1.2 channels. Science. United States; 2010;330: 105–109. doi:10.1126/science.1191086
10. Nguyen N, Biet M, Simard É, Béliveau É, Francoeur N, Guillemette G, et al. STIM1 participates in the contractile rhythmicity of HL-1 cells by moderating T-type Ca2+ channel activity. Biochim Biophys Acta - Mol Cell Res. 2013;1833: 1294–1303. doi:https://doi.org/10.1016/j.bbamcr.2013.02.027
11. Jékely G. Global view of the evolution and diversity of metazoan neuropeptide signaling. Proc Natl Acad Sci. 2013;110: 8702 LP-8707. Available: http://www.pnas.org/content/110/21/8702.abstract
12. Elphick MR, Mirabeau O, Larhammar D. Evolution of neuropeptide signalling systems. J Exp Biol. 2018;221: jeb151092. doi:10.1242/jeb.151092
13. Nassel DR, Winther AM. Drosophila neuropeptides in regulation of physiology and behavior. Prog Neurobiol. 2010;92: 42–104. Available: http://www.ncbi.nlm.nih.gov/entrez/query.fcgi?cmd=Retrieve&db=PubMed&dopt=Citation&list_uids=20447440

14. Taghert PH, Nitabach MN. Peptide neuromodulation in invertebrate model systems. Neuron. United States; 2012;76: 82–97. doi:10.1016/j.neuron.2012.08.035
15. Venkiteswaran G, Hasan G. Intracellular Ca2+ signaling and store-operated Ca2+ entry are required in Drosophila neurons for flight. Proc Natl Acad Sci U S A. 2009;106: 10326–10331. Available: http://www.ncbi.nlm.nih.gov/entrez/query.fcgi?cmd=Retrieve&db=PubMed&dopt=Citation&list_uids=19515818
16. Chakraborty S, Deb BK, Chorna T, Konieczny V, Taylor CW, Hasan G. Mutant IP3 receptors attenuate store-operated Ca2+ entry by destabilizing STIM-Orai interactions in Drosophila neurons. J Cell Sci. 2016; doi:10.1242/jcs.191585
17. Richhariya S, Jayakumar S, Kumar Sukumar S, Hasan G. dSTIM and Ral/Exocyst Mediated Synaptic Release from Pupal Dopaminergic Neurons Sustains Drosophila Flight. eneuro. 2018;5. Available: http://eneuro.org/content/early/2018/05/22/ENEURO.0455-17.2018.abstract
18. Jayakumar S, Richhariya S, Deb BK, Hasan G. A Multicomponent Neuronal Response Encodes the Larval Decision to Pupariate upon Amino Acid Starvation. J Neurosci. 2018;38: 10202 LP-10219. doi:10.1523/JNEUROSCI.1163-18.2018
19. Agrawal N, Venkiteswaran G, Sadaf S, Padmanabhan N, Banerjee S, Hasan G. Inositol 1,4,5-trisphosphate receptor and dSTIM function in Drosophila insulin-producing neurons regulates systemic intracellular calcium homeostasis and flight. J Neurosci. 2010;30: 1301–1313. Available: http://www.ncbi.nlm.nih.gov/entrez/query.fcgi?cmd=Retrieve&db=PubMed&dopt=Citation&list_uids=20107057
20. Chakraborty S, Hasan G. IP3R, store-operated Ca2+ entry and neuronal Ca2+ homoeostasis in Drosophila. Biochem Soc Trans. 2012/01/21. 2012;40: 279–281. doi:10.1042/BST20110618BST20110618 [pii]
21. Gopurappilly R, Deb BK, Chakraborty P, Hasan G. Stable STIM1 Knockdown in Self-Renewing Human Neural Precursors Promotes Premature Neural Differentiation [Internet]. Frontiers in Molecular Neuroscience . 2018. p. 178. Available: https://www.frontiersin.org/article/10.3389/fnmol.2018.00178
22. Megha, Hasan G. IP3R-mediated Ca2+ release regulates protein metabolism in Drosophila neuroendocrine cells: implications for development under nutrient stress. Development. England; 2017;144: 1484–1489. doi:10.1242/dev.145235
23. Agrawal T, Sadaf S, Hasan G. A genetic RNAi screen for IP(3)/Ca(2)(+) coupled GPCRs in Drosophila identifies the PdfR as a regulator of insect flight. PLoS Genet. 2013/10/08. 2013;9: e1003849. doi:10.1371/journal.pgen.1003849PGENETICS-D-13-01291 [pii]
24. Nassel DR, Enell LE, Santos JG, Wegener C, Johard HA. A large population of diverse neurons in the Drosophila central nervous system expresses short neuropeptide F, suggesting multiple distributed peptide functions. BMC Neurosci. 2008;9: 90. Available: http://www.ncbi.nlm.nih.gov/entrez/query.fcgi?cmd=Retrieve&db=PubMed&dopt=Citation&list_uids=18803813
25. Rhea JM, Wegener C, Bender M. The proprotein convertase encoded by amontillado (amon) is required in Drosophila corpora cardiaca endocrine cells producing the glucose regulatory hormone AKH. PLoS Genet. 2010;6: e1000967. Available: http://www.ncbi.nlm.nih.gov/entrez/query.fcgi?cmd=Retrieve&db=PubMed&dopt=C

itation&list_uids=20523747

26. Pathak T, Agrawal T, Richhariya S, Sadaf S, Hasan G. Store-Operated Calcium Entry through Orai Is Required for Transcriptional Maturation of the Flight Circuit in Drosophila. J Neurosci. United States; 2015;35: 13784–13799. doi:10.1523/JNEUROSCI.1680-15.2015

27. Lee KS, You KH, Choo JK, Han YM, Yu K. Drosophila short neuropeptide F regulates food intake and body size. J Biol Chem. 2004;279: 50781–50789. Available: http://www.ncbi.nlm.nih.gov/entrez/query.fcgi?cmd=Retrieve&db=PubMed&dopt=Citation&list_uids=15385546

28. Subramanian M, Jayakumar S, Richhariya S, Hasan G. Loss of IP3 receptor function in neuropeptide secreting neurons leads to obesity in adult Drosophila. BMC Neurosci. 2013/12/20. 2013;14: 157. doi:10.1186/1471-2202-14-1571471-2202-14-157 [pii]

29. Agrawal N, Padmanabhan N, Hasan G. Inositol 1,4,5- trisphosphate receptor function in Drosophila insulin producing cells. PLoS One. 2009;4: e6652. Available: http://www.ncbi.nlm.nih.gov/entrez/query.fcgi?cmd=Retrieve&db=PubMed&dopt=Citation&list_uids=19680544

30. Choi YJ, Lee G, Hall JC, Park JH. Comparative analysis of Corazonin-encoding genes (Crz's) in Drosophila species and functional insights into Crz-expressing neurons. J Comp Neurol. United States; 2005;482: 372–385. doi:10.1002/cne.20419

31. Rao S, Lang C, Levitan ES, Deitcher DL. Visualization of neuropeptide expression, transport, and exocytosis in Drosophila melanogaster. J Neurobiol. United States; 2001;49: 159–172.

32. Fosque BF, Sun Y, Dana H, Yang C-T, Ohyama T, Tadross MR, et al. Neural circuits. Labeling of active neural circuits in vivo with designed calcium integrators. Science. United States; 2015;347: 755–760. doi:10.1126/science.1260922

33. Veenstra JA. Peptidergic paracrine and endocrine cells in the midgut of the fruit fly maggot. Cell Tissue Res. 2009;336: 309–323. Available: http://www.ncbi.nlm.nih.gov/entrez/query.fcgi?cmd=Retrieve&db=PubMed&dopt=Citation&list_uids=19319573

34. Wegener C, Herbert H, Kahnt J, Bender M, Rhea JM. Deficiency of prohormone convertase dPC2 (AMONTILLADO) results in impaired production of bioactive neuropeptide hormones in Drosophila. J Neurochem. 2011;118: 581–595. Available: http://www.ncbi.nlm.nih.gov/entrez/query.fcgi?cmd=Retrieve&db=PubMed&dopt=Citation&list_uids=21138435

35. Luo J, Liu Y, Nassel DR, Nässel DR. Insulin/IGF-regulated size scaling of neuroendocrine cells expressing the bHLH transcription factor Dimmed in Drosophila. PLoS Genet. 2014/01/05. Public Library of Science; 2013;9: e1004052. doi:10.1371/journal.pgen.1004052

36. Park D, Veenstra JA, Park JH, Taghert PH. Mapping peptidergic cells in Drosophila: where DIMM fits in. PLoS One. 2008;3: e1896. Available: http://www.ncbi.nlm.nih.gov/entrez/query.fcgi?cmd=Retrieve&db=PubMed&dopt=Citation&list_uids=18365028

37. Richhariya S, Jayakumar S, Abruzzi K, Rosbash M, Hasan G. A pupal transcriptomic screen identifies Ral as a target of store-operated calcium entry in Drosophila neurons. Sci Rep. The Author(s); 2017;7: 42586. Available: http://dx.doi.org/10.1038/srep42586

38. Wong MY, Cavolo SL, Levitan ES. Synaptic neuropeptide release by dynamin-

dependent partial release from circulating vesicles. Mol Biol Cell. United States; 2015;26: 2466–2474. doi:10.1091/mbc.E15-01-0002

39. McNabb SL, Truman JW. Light and peptidergic eclosion hormone neurons stimulate a rapid eclosion response that masks circadian emergence in Drosophila. J Exp Biol. 2008;211: 2263–2274. doi:10.1242/jeb.015818

40. Klose M, Duvall L, Li W, Liang X, Ren C, Steinbach JH, et al. Functional PDF Signaling in the Drosophila Circadian Neural Circuit Is Gated by Ral A-Dependent Modulation. Neuron. 2016/05/05. 2016;90: 781–794. doi:10.1016/j.neuron.2016.04.002

41. Nässel DR. Neuropeptide signaling near and far: how localized and timed is the action of neuropeptides in brain circuits? Invertebr Neurosci. 2009;9: 57. doi:10.1007/s10158-009-0090-1

42. Kubrak OI, Lushchak O V, Zandawala M, Nässel DR. Systemic corazonin signalling modulates stress responses and metabolism in Drosophila. Open Biol. The Royal Society; 2016;6: 160152. doi:10.1098/rsob.160152

43. Chintapalli VR, Wang J, Dow JAT. Using FlyAtlas to identify better Drosophila melanogaster models of human disease. Nat Genet. United States; 2007;39: 715–720. doi:10.1038/ng2049

44. Pulver SR, Pashkovski SL, Hornstein NJ, Garrity PA, Griffith LC. Temporal dynamics of neuronal activation by Channelrhodopsin-2 and TRPA1 determine behavioral output in Drosophila larvae. J Neurophysiol. 2009/04/01. American Physiological Society; 2009;101: 3075–3088. doi:10.1152/jn.00071.2009

45. Dawydow A, Gueta R, Ljaschenko D, Ullrich S, Hermann M, Ehmann N, et al. Channelrhodopsin-2–XXL, a powerful optogenetic tool for low-light applications. Proc Natl Acad Sci. 2014;111: 13972 LP-13977. Available: http://www.pnas.org/content/111/38/13972.abstract

46. Lee G, Kim KM, Kikuno K, Wang Z, Choi YJ, Park JH. Developmental regulation and functions of the expression of the neuropeptide corazonin in Drosophila melanogaster. Cell Tissue Res. 2008;331: 659–673. Available: http://www.ncbi.nlm.nih.gov/entrez/query.fcgi?cmd=Retrieve&db=PubMed&dopt=Citation&list_uids=18087727

47. Kapan N, Lushchak O V, Luo J, Nässel DR. Identified peptidergic neurons in the Drosophila brain regulate insulin-producing cells, stress responses and metabolism by coexpressed short neuropeptide F and corazonin. Cell Mol Life Sci. 2012;69: 4051–4066. doi:10.1007/s00018-012-1097-z

48. Johnson EC, Kazgan N, Bretz CA, Forsberg LJ, Hector CE, Worthen RJ, et al. Altered Metabolism and Persistent Starvation Behaviors Caused by Reduced AMPK Function in Drosophila. Hassan BA, editor. PLoS One. San Francisco, USA: Public Library of Science; 2010;5: e12799. doi:10.1371/journal.pone.0012799

49. Tayler TD, Pacheco DA, Hergarden AC, Murthy M, Anderson DJ. A neuropeptide circuit that coordinates sperm transfer and copulation duration in Drosophila. Proc Natl Acad Sci U S A. National Academy of Sciences; 2012;109: 20697–20702. doi:10.1073/pnas.1218246109

50. McClure KD, Heberlein U. A Small Group of Neurosecretory Cells Expressing the Transcriptional Regulator apontic and the Neuropeptide corazonin Mediate Ethanol Sedation in Drosophila. J Neurosci. Society for Neuroscience; 2013;33: 4044–4054. doi:10.1523/JNEUROSCI.3413-12.2013

51. Sha K, Choi S-H, Im J, Lee GG, Loeffler F, Park JH. Regulation of Ethanol-Related

Behavior and Ethanol Metabolism by the Corazonin Neurons and Corazonin Receptor in Drosophila melanogaster. PLoS One. Public Library of Science; 2014;9: e87062. Available: https://doi.org/10.1371/journal.pone.0087062

52. Lee KS, Kwon OY, Lee JH, Kwon K, Min KJ, Jung SA, et al. Drosophila short neuropeptide F signalling regulates growth by ERK-mediated insulin signalling. Nat Cell Biol. 2008;10: 468–475. Available: http://www.ncbi.nlm.nih.gov/entrez/query.fcgi?cmd=Retrieve&db=PubMed&dopt=Citation&list_uids=18344986

53. Selcho M, Millán C, Palacios-Muñoz A, Ruf F, Ubillo L, Chen J, et al. Central and peripheral clocks are coupled by a neuropeptide pathway in Drosophila. Nat Commun. The Author(s); 2017;8: 15563. Available: http://dx.doi.org/10.1038/ncomms15563

54. Chen W, Shi W, Li L, Zheng Z, Li T, Bai W, et al. Regulation of sleep by the short neuropeptide F (sNPF) in Drosophila melanogaster. Insect Biochem Mol Biol. England; 2013;43: 809–819. doi:10.1016/j.ibmb.2013.06.003

55. Shang Y, Donelson NC, Vecsey CG, Guo F, Rosbash M, Griffith LC. Short neuropeptide F is a sleep-promoting inhibitory modulator. Neuron. United States; 2013;80: 171–183. doi:10.1016/j.neuron.2013.07.029

56. Veenstra JA. Does corazonin signal nutritional stress in insects? Insect Biochem Mol Biol. 2009;39: 755–762. Available: http://www.ncbi.nlm.nih.gov/entrez/query.fcgi?cmd=Retrieve&db=PubMed&dopt=Citation&list_uids=19815069

57. Mishra D, Miyamoto T, Rezenom YH, Broussard A, Yavuz A, Slone J, et al. The Molecular Basis of Sugar Sensing in Drosophila Larvae. Curr Biol. Elsevier; 2013;23: 1466–1471. doi:10.1016/j.cub.2013.06.028

58. Miyamoto T, Amrein H. Diverse roles for the Drosophila fructose sensor Gr43a. Fly (Austin). Landes Bioscience; 2014;8: 19–25. doi:10.4161/fly.27241

59. Johnson EC, Shafer OT, Trigg JS, Park J, Schooley DA, Dow JA, et al. A novel diuretic hormone receptor in Drosophila: evidence for conservation of CGRP signaling. J Exp Biol. England; 2005;208: 1239–1246. doi:10.1242/jeb.01529

60. Hartenstein V. The neuroendocrine system of invertebrates: a developmental and evolutionary perspective. J Endocrinol. England; 2006;190: 555–570. doi:10.1677/joe.1.06964

61. Onaka T, Takayanagi Y, Leng G. Metabolic and stress-related roles of prolactin-releasing peptide. Trends Endocrinol Metab. 2010;21: 287–293. doi:https://doi.org/10.1016/j.tem.2010.01.005

62. van den Pol AN. Neuropeptide transmission in brain circuits. Neuron. United States; 2012;76: 98–115. doi:10.1016/j.neuron.2012.09.014

63. Shakiryanova D, Zettel GM, Gu T, Hewes RS, Levitan ES. Synaptic neuropeptide release induced by octopamine without Ca2+ entry into the nerve terminal. Proc Natl Acad Sci U S A. 2011;108: 4477–4481. Available: http://www.ncbi.nlm.nih.gov/entrez/query.fcgi?cmd=Retrieve&db=PubMed&dopt=Citation&list_uids=21368121

64. Wang Y, Wu Q, Hu M, Liu B, Chai Z, Huang R, et al. Ligand- and voltage-gated Ca^{2+} channels differentially regulate the mode of vesicular neuropeptide release in mammalian sensory neurons. Sci Signal. 2017;10: eaal1683. Available: http://stke.sciencemag.org/content/10/484/eaal1683.abstract

840 65. Zhou Q, Yen A, Rymarczyk G, Asai H, Trengrove C, Aziz N, et al. Impairment of
841 PARK14-dependent Ca(2+) signalling is a novel determinant of Parkinson's disease.
842 Nat Commun. England; 2016;7: 10332. doi:10.1038/ncomms10332
843 66. Secondo A, Bagetta G, Amantea D. On the Role of Store-Operated Calcium Entry in
844 Acute and Chronic Neurodegenerative Diseases. Front Mol Neurosci. Switzerland;
845 2018;11: 87. doi:10.3389/fnmol.2018.00087
846 67. Popugaeva E, Bezprozvanny I. Role of endoplasmic reticulum Ca2+ signaling in the
847 pathogenesis of Alzheimer disease. Front Mol Neurosci. Switzerland; 2013;6: 29.
848 doi:10.3389/fnmol.2013.00029
849 68. Wegener C, Neupert S, Predel R. Direct MALDI-TOF mass spectrometric peptide
850 profiling of neuroendocrine tissue of Drosophila. Methods Mol Biol. 2010;615: 117–
851 127. Available:
852 http://www.ncbi.nlm.nih.gov/entrez/query.fcgi?cmd=Retrieve&db=PubMed&dopt=C
853 itation&list_uids=20013204
854
855